Title

Electrochemical potential enables dormant spores to integrate environmental signals.

Journal

Science, 378(6615)

Authors

Kikuchi, Kaito
Galera-Laporta, Leticia
Weatherwax, Colleen
et al.

Publication Date

2022-10-07

DOI

10.1126/science.abl7484

Peer reviewed

HHS Public Access

Author manuscript

Science. Author manuscript; available in PMC 2023 October 23.

Published in final edited form as:

Science. 2022 October 07; 378(6615): 43–49. doi:10.1126/science.abl7484.

Electrochemical potential enables dormant spores to integrate environmental signals

Kaito Kikuchi[1,†], **Leticia Galera-Laporta**[1,†], **Colleen Weatherwax**[1], **Jamie Y Lam**[2], **Eun Chae Moon**[1], **Emmanuel A Theodorakis**[2], **Jordi Garcia-Ojalvo**[3,6], **Gürol M Süel**[1,4,5,6,*]

[1]Molecular Biology Section, Division of Biological Sciences, University of California San Diego; La Jolla, CA 92093, USA

[2]Department of Chemistry and Biochemistry, University of California San Diego; La Jolla, CA 92093, USA

[3]Department of Medicine and Life Sciences, Universitat Pompeu Fabra; 08003 Barcelona, Spain

[4]San Diego Center for Systems Biology, University of California San Diego; La Jolla, CA 92093-0380, USA

[5]Center for Microbiome Innovation, University of California San Diego; La Jolla, CA 92093-0380, USA

[6]Senior author

Abstract

The dormant state of bacterial spores is generally thought to be devoid of biological activity. We show that despite continued dormancy, spores can integrate environmental signals over time through a pre-existing electrochemical potential. Specifically, we studied thousands of individual *Bacillus subtilis* spores that remain dormant when exposed to transient nutrient pulses. Guided by a mathematical model of bacterial electrophysiology, we modulated the decision to exit dormancy by genetically and chemically targeting potassium ion flux. We confirmed that short nutrient pulses result in step-like changes in the electrochemical potential of persistent spores. During dormancy, spores thus gradually release their stored electrochemical potential to integrate extracellular information over time. These findings reveal a decision-making mechanism that operates in physiologically inactive cells.

*Correspondence: gsuel@ucsd.edu.
†These authors contributed equally

Author contributions:
Conceptualization: KK, LGL, CW, JGO, GMS
Methodology: KK, LGL, CW, JGO, GMS
Experiments: LGL, KK, ECM
Design, synthesis, and characterization of the charge-neutral version of Thioflavin-T: JYL, EAT
Experimental data analysis: KK, LGL, ECM
Mathematical modeling: CW, JGO
Funding acquisition: GMS, JGO, EAT
Supervision: GMS, JGO, EAT
Project administration: GMS
Writing: GMS, KK, LGL, CW, JGO, ECM, JYL, EAT

Competing interests:
The authors declare that they have no competing interests.

One-Sentence Summary:

Bacterial spores use an integrate-and-fire mechanism to monitor external conditions during dormancy.

Main Text:

The formation of bacterial spores (sporulation) is a common and well-characterized survival strategy in many microbial species (1, 2). Spores are partially dehydrated cells enclosed by a protective coat that can survive environmental extremes and remain dormant for years (3). They need to be robust to environmental fluctuations to avoid exiting their dormant state (germinating) prematurely. At the same time, spores need to germinate if they detect favorable conditions (4) (Fig. 1A). Germination requires the re-hydration of the spore which is promoted by the release of Calcium-Dipicolinic Acid (CaDPA) (5). Aside from degradation of RNA immediately after sporulation (6), dormant spores appear to have no measurable metabolic or biological activity (7). Therefore, it remains unclear whether dormant spores possess any activity that could affect the choice of whether or not to germinate. We thus tested whether dormant *Bacillus subtilis* spores experience any physiological changes in response to subtle environmental signals that do not trigger germination. Addressing these questions could reveal how spores reconcile their robust dormant state with the need to process extracellular information and make an informed decision on whether to continue or exit their dormancy.

Spores can be pre-treated with nutrients to promote germination (8–10). These findings imply that spores can somehow integrate extracellular signals despite their dormancy, and thereby alter their future likelihood of triggering germination. While there are no well-established mechanisms for dormant cells to integrate extracellular information, the ability of spores to modulate their future response suggests a conceptual similarity to a decision-making mechanism in neuroscience known as integrate-and-fire (11, 12). This mechanism describes how neurons respond to small synaptic inputs before reaching the threshold that triggers an action potential (13). It is unclear whether dormant spores employ a similar mechanism to process environmental inputs and modulate their approach towards a threshold that triggers germination.

Given the physiological inactivity of spores, we investigated a possible integration mechanism based on passive ion flux, which does not require cellular energy. Our findings indicate that physiologically inactive spores integrate environmental signals by modifying pre-existing ion gradients that were established during sporulation. Dormant spores can thus use stored electrochemical potential energy to regulate their cell-fate decision without requiring de-novo ATP synthesis. In this way, spores can alter their distance to the germination threshold depending on environmental inputs, while still in the dormant state. This mechanism also reconciles the robust dormancy of spores with the ability to gradually become sensitized to future environmental signals.

Results:

Bacillus subtilis spores can remain dormant despite exposure to germinant pulses

We confirmed that similar to laboratory strains, undomesticated *Bacillus subtilis* spores can be pre-treated with short nutrient (germinant) pulses to increase the likelihood of germination (8). Specifically, we imaged spores (Fig. 1B) within a microfluidic device that allows single-cell monitoring and precise control over the components in the incubation medium (see Methods). We optically tracked the switch in phase-contrast brightness that results from the re-hydration of spores during germination (4, 14) (Fig. 1C, Fig. S1A and B). Using this experimental approach, we exposed thousands of spores to a single short germinant pulse (10 mM L-alanine for 3 minutes), and found that ~95% of spores remained dormant (95.2% ± 1.9%, n = 2,244; Fig. 1D). We used the germinant L-alanine because it is a naturally occurring nutrient that triggers germination through designated receptors in bacterial spores (15). Spores that did not germinate upon stimulation remained dormant for at least the next 20 hours of imaging (Fig. S1C). Any spore that did germinate in response to the germinant pulse did so on average within 15 minutes (14.85 ± 1.07, n = 1,831; Fig. S1D).

To quantify the integration capacity of spores, we applied a second germinant pulse, separated by 2 hours from the first pulse to ensure that germination in response to the first pulse of germinant had subsided. After the second pulse, approximately half of the remaining spores germinated (52.1% ± 6.2%). The germination propensity of spores was independent of their location within the microfluidic chamber (Fig. S2). We defined the spore's integration capacity as the population-level change (difference) in the germination probability in response to two consecutive germinant pulses (Fig. 1E). The germination probability increased by 47% ± 1% (mean ± SD, N=9 replicate populations) between the first and second pulse. Spores thus become sensitized by the first exposure and appear to move closer towards a germination threshold.

A mathematical model of the role of ion flux in responding to germinant pulses

To explain how physiologically inactive spores could integrate information about germinant exposure over time, we explored an ion flux as a mechanism, since this process could occur passively with pre-existing ionic gradients established during sporulation. Other processes such as de-novo gene expression and enzymatic activity typically require energy, which is highly limited in spores. In particular, we focused here on the flux of potassium, since it is the most abundant intracellular ion in bacteria, and has physiological roles in the stress response of *B. subtilis* (16–19). Furthermore, potassium ions have been proposed to stabilize the formation of bacterial spores (20). To investigate the possible role of potassium ion flux in dormant spores, we developed a mathematical model based on the Hodgkin-Huxley (HH) framework (21) (Fig. 1F, Box 1, and Supplementary Text). Our model describes how potassium ion flux can drive a spore towards a fixed germination threshold through an integrate-and-fire mechanism, without requiring any physiological activity.

Our mathematical model assumes that potassium ions enter or leave a spore through passive transport through both selective potassium channels and non-specific ion channels. The

direction and rate of potassium flux across the spore membrane depend on the potassium ion concentration gradient, as well as on the membrane potential of the spore (16–19) (see Supplementary Text). We assume that spores contain high amounts of potassium (22, 23), which would result in ion efflux when channels are open. We also assume that ion pumps are inactive during dormancy, given that they require ATP for transport, which is highly limited and not actively produced in spores (6). Furthermore, the model assumes that ion channels (both potassium specific and non-specific) are closed until germinant is added. The channels open in the presence of germinant and close in its absence. Finally, we assume that the initial potassium content of spores has some variability, and that germination begins when a spore's internal potassium concentration drops below a certain value (that is, it reaches the germination threshold, Fig. 1G and H). Given these assumptions, the model predicts that, when exposed to consecutive short germinant pulses, few spores germinate during the first pulse, whereas most spores do so during the second, or subsequent pulses (Fig. 1I). This increase in the germination probability of spores is consistent with our experimental observations (Fig. 1D). Different germinant concentrations in the first pulse did not markedly change the fraction of germinated spores (Fig. S3). In contrast, the germinated fraction increased with higher concentration of L-alanine in the second pulse. This difference in the sensitivity of spores to the first and second germinant pulse concentrations further demonstrates integration of information. Efflux of potassium from dormant spores was also confirmed with an extracellular potassium indicator, Asante Potassium Green-4 tetramethylammonium salt (APG-4 TMA) (Fig. S4A and B). Our modeling approach thus shows how spores might use intracellular potassium concentration to integrate information about previous germinant exposures and change their sensitivity to future exposures.

Initial potassium concentrations define the distance to the germination threshold

Our mathematical model assumes that the initial potassium content defines the distance to the germination threshold (Fig. 1G and H). To test this, we generated a mutant strain in which the KtrC subunit of the KtrCD potassium importer was deleted, which is expected to lower intracellular potassium content and, consequently put the spore closer to the threshold compared to wild-type spores (Fig. 2A). KtrC is the major potassium importer expressed in the inner spore membrane during the sporulation process (24), enabling potassium uptake (25, 26) (Fig. 2B and C). By generating spores in the presence of an intracellular potassium indicator, Asante Potassium Green-4 Acetoxymethyl ester (APG-4 AM), we confirmed that the *ΔktrC* spores contain less potassium than do wild-type spores (Fig. S4C through F). Accordingly, the *ΔktrC* spores are mathematically predicted to be more likely to germinate in response to the first germinant pulse (Fig. 2D). Indeed, measurements show that 42% of the *ΔktrC* spores germinated after the first pulse, compared to 5% of the wild-type spores (Fig. 2E through G, Movie S1). The germinated fraction of *ΔktrC* spores then further increased after the second pulse (Fig. 2H). We obtained similar results with spores lacking KtrD, the other subunit of the KtrCD potassium importer (Fig. S5A).

Given the high germination probability of *ΔktrC* spores, almost the entire population (~94%) exited the dormant state after only two germinant pulses (Fig. 2G). However, because the deletion of KtrC does not affect potassium efflux in spores, the integration capacity of *ΔktrC*

spores is comparable to that of wild-type spores (Fig. 2I). To further confirm that the lower potassium content of *ΔktrC* spores caused the higher sensitivity to germinant pulses, we supplied additional potassium during sporulation of *ΔktrC* cells. Increasing the potassium content in *ΔktrC* spores should increase their distance to the germination threshold, which in turn would be reflected in a decrease in their germination probability (Fig. S5B). In agreement with those expectations, the addition of 150 mM of potassium in the sporulation medium resulted in *ΔktrC* spores that responded to germinant pulses similarly to wild-type spores (Fig. S5C and D). These results are consistent with the modeling prediction and support the idea that the initial intracellular potassium concentration of spores specifically defines their distance to the germination threshold.

Potassium ion channels contribute to the integration capacity of spores

We investigated the modeling prediction that spores use potassium efflux to integrate over consecutive germinant pulses. To this end, we studied a mutant strain lacking the YugO potassium ion channel (27) (Fig. 3A and B). We confirmed that *ΔyugO* spores contain less potassium than do wild-type spores with the intracellular potassium indicator APG-4 AM (Fig. S4C through F). Therefore, the *ΔyugO* spores should be initially closer to the germination threshold and be more sensitive than wild-type spores to the first germinant pulse (Fig. 3A through D). On the other hand, the absence of the YugO channel also implies a reduced potassium efflux in response to germinant pulses. According to our model, such reduced potassium efflux in germinant-exposed spores should lower their integration capacity, and thus the germination probability for subsequent germinant pulses would be lower (Fig. 3D). In other words, the *ΔyugO* spores would not markedly increase their sensitivity to consecutive germinant pulses, which should distinguish this strain from the wild-type and the *ΔktrC* strains. These mutant spores are therefore predicted to approach the germination threshold more gradually due to reduced potassium efflux.

We experimentally tested these predictions. Essentially, the progression of the wild-type and the *ΔyugO* spores towards the germination threshold are predicted to exhibit a cross-over point (Fig. 3D). Experiments confirmed that the *ΔyugO* spores have a higher response than wild-type to the first germinant pulse (with 30% vs 5% of the spores germinating, respectively) (Fig. 3E,F,H, Movie S2). However, these spores lacked the increase in germination probability in response to subsequent pulses exhibited by the wild-type spores (Fig. 3I). This in turn reflects a substantial loss in integration capacity of the *ΔyugO* spores when compared to wild-type (Fig. 3J, Fig. S6). The phenotype of the *ΔyugO* spores (high initial germination probability, and low integration capacity) is thus consistent with our modeling predictions. Importantly, the *ΔyugO* strain also indicates that reduced efflux of potassium decreases the integration capacity of spores. These results suggest that potassium efflux serves as an integration mechanism that modulates the approach to the germination threshold.

Given the complex phenotype of the *ΔyugO* strain, we turned to chemical perturbations of potassium flux in wild-type spores to independently determine whether potassium flux underlies the integration capacity of spores. We confirmed that modifying the external potassium concentration changed the integration capacity of wild-type spores (Fig. S6).

Specifically, the absence of potassium in the medium, expected to promote higher potassium efflux in spores, increased the integration capacity (from 0.47 ± 0.01 to 0.63 ± 0.02). In contrast, increasing extracellular potassium concentration lowered the integration capacity (RM + 600 mM KCl: 0.32 ± 0.01; RM + 1 M KCl: 0.03 ± 0.01). To test whether reduction in integration capacity might result from increased osmotic stress, we showed that adding 1 M sorbitol had no effect on integration capacity (RM + 1 M sorbitol: 0.44 ± 0.02). The electrochemical gradient of potassium thus influences the integration capacity of spores.

We also tested how the integration capacity of wild-type spores is affected by blocking potassium channels with the drug quinine (1 mM; Fig. 3A through C, Figs. S4B, S6) (28–31). According to our model, such blocking of potassium channels is expected to specifically reduce the germination probability in response to consecutive germinant pulses (Fig. 3D). In agreement with this prediction, treatment of spores with quinine reduced the response of wild-type spores to the second germinant pulse, with around 80% of the spores remaining dormant, in comparison with around 45% in the absence of the drug (Fig. 3G, H, I, Movie S3). These results support the proposed integrate-and-fire mechanism by showing that similar to the deletion of the YugO channel, chemical blocking of potassium efflux in wild-type spores also impairs their integration capacity (Fig. 3J, Fig. S6).

Changes in the electrochemical potential of dormant spores

Our mathematical model proposes that the flux of potassium ions driving the processing of information during dormancy is modulated by the electrochemical potential of the spores. According to the integrate-and-fire mechanism, spores that are further from their germination threshold would require multiple germinant pulses to reach the threshold, each pulse causing an incremental electrochemical potential change (Fig. 4A). Specifically, the transient efflux of potassium cations triggered by germinant pulses is mathematically predicted to increase the negative electrochemical potential of spores in a step-like manner, even when the pulses do not trigger germination (Fig. 4B). To test this prediction, we used a previously characterized cationic fluorescent dye (Thioflavin-T, ThT) to measure changes in the electrochemical potential of dormant spores (see Methods) (16, 32). As spores are notoriously impermeable to most chemicals (33), we expected that peripheral staining by ThT would reflect the spore's overall negative electrochemical potential (20).

To experimentally test our modeling prediction of electrochemical potential jumps, we tracked thousands of individual wild-type spores over time and simultaneously imaged phase-contrast and ThT fluorescence intensities (Fig. 4C through F). Spores that did not trigger germination exhibited sudden changes in their electrochemical potential in response to germinant pulses (Movie S4). Spores that required multiple germinant pulses to trigger germination exhibited a multi-step progression before reaching their germination threshold. These increases in the ThT signal were not due to increased spore permeability, as ThT continued to stain the spore's periphery and did not transition to its interior (Fig. 4D, Movie S4). Therefore, accumulation of ThT on the spore periphery appears to reflect changes in the ionic content of the spore. We observed no characteristic changes of the phase-contrast brightness of dormant spores during the increases in the ThT signal (Fig. S7A). We also tested L-valine, another naturally occurring germinant (34), and

observed similar changes in ThT signal (Fig. S7B). Furthermore, we used another positively charged dye, Tetramethylrhodamine methyl ester (TMRM), commonly used to measure the electrochemical potential of cells (35). TMRM also stained the periphery of spores, and increases in the TMRM signal amplitude were qualitatively similar to those measured with ThT (Fig. S8A and B). To validate that the observed jumps in fluorescence during germinant additions were not simply a staining artifact, we synthesized a charge-neutral version of ThT (Fig. 4E inset, Figs. S8C and D, S9, Methods, and Supplementary Text). Although this charge-neutral ThT dye also stained the spore periphery, we observed no increases in the signal amplitude during germinant pulses. Instead, the fluorescence signal of the neutral ThT dye monotonically decayed over time likely due to photobleaching. To exclude the possibility that the observed changes in electrochemical potential could be related to the release of CaDPA during the initiation of germination, we generated a mutant strain lacking a subunit of the SpoVA channel, namely SpoVAF (Fig. S10A). This subunit is essential for effective CaDPA release during germination, and its deletion causes a delay in germination (36). Deletion of SpoVAF slowed the response time of spores to L-alanine (Fig. S10B). However, loss of *spoVAF* did not impact the electrochemical potential changes we observed in spores (Fig. S10C and D), indicating that CaDPA release is not required for the integration of information in dormant spores. Together, these results demonstrate that germinant pulses cause sudden changes in the electrochemical potential of spores that otherwise remain dormant. As predicted, spores that required multiple germinant pulses to initiate germination also exhibited multiple jumps in their electrochemical potential, indicating their greater distance to the germination threshold. The ability to visualize and observe a multi-step and gradual approach of dormant spores towards their germination threshold provides further evidence in support of the integrate-and-fire mechanism.

We investigated whether the integration capacity that we determined from population-level statistics correlated with the independently observed jumps in the electrochemical potential of individual spores. In particular, a higher integration capacity should correlate with a higher change in electrochemical potential. We therefore measured germinant-induced changes in the electrochemical potential for thousands of spores obtained from various perturbations considered in this study (Fig. 4F and G). Higher integration capacity correlated with a higher average increase in electrochemical potential (Fig. 4H). Specifically, wild-type and *ΔktrC* spores, which have similarly high changes in electrochemical potential, also exhibited relatively higher integration capacities. Furthermore, the *ΔyugO* and the quinine-exposed wild-type spores, which both exhibited lower average changes in their electrochemical potential, had reduced integration capacities. These findings support the prediction that dormant spores integrate environmental information through ion flux-induced changes in their electrochemical potential.

Discussion:

We studied how physiologically inactive spores detect and respond to transient germinant pulses. Our results reveal that despite their dormancy, spores can integrate extracellular information and alter their intrinsic state. This ability to process information appears to be supported by pre-existing ionic gradients generated during sporulation. In this way, dormant spores can reach the decision to initiate germination by using electrochemical potential

energy, rather than requiring a source of cellular energy, such as ATP. Spores may thus be analogous to a biological capacitor, in that they store and utilize an electrochemical potential to move closer to the germination threshold (Fig. 4I). The integrate-and-fire model proposed here provides both a conceptual and mechanistic explanation for how spores can respond to an environmental signal despite being physiologically inactive. The ability to sum inputs over time prior to reaching a threshold ensures that germination is triggered only when favorable conditions persist, while also ignoring small environmental fluctuations. While the integrate-and-fire model is used to describe how neurons process information, our work suggests that this concept may represent a more general solution to the need for information-processing in diverse biological systems including energy-limited cells.

Supplementary Material

Refer to Web version on PubMed Central for supplementary material.

Acknowledgements:

We acknowledge Munehiro Asally, Tolga Çağatay, Joseph Larkin, Colin Comerci, and Katherine Süel for helpful discussions; Wade Winkler and David Kearns for kindly providing bacterial strains; and Jacqueline Humphries for help with strain construction.

Funding:

National Institute of General Medical Sciences grant R01 GM121888 (GMS)

National Institute of General Medical Sciences grant R35 GM139645 (GMS)

Howard Hughes Medical Institute-Simons Foundation Faculty Scholars Program (GMS)

Spanish Ministry of Science, Innovation and Universities Project PGC2018–101251-B-I00 (JGO)

FEDER CEX2018–000792-M (JGO)

Generalitat de Catalunya ICREA Academia programme (JGO)

ANRI Fellowship (KK)

National Institute on Aging grant RF1 AG062362 (EAT)

Data and materials availability:

All data are available in the manuscript or the supplementary material. All bacterial strains and material generated in this study are available from the authors. Code for the mathematical model and for generating the germination cumulative density functions are available at https://github.com/suellab/Kikuchi_Galera-Laporta_2022 (37).

References and Notes:

1. Stragier P, Losick R, Molecular genetics of sporulation in Bacillus subtilis. Genetics. 30, 297–341 (1996).
2. Piggot PJ, Hilbert DW, Sporulation of Bacillus subtilis. Curr. Opin. Microbiol. 7, 579–586 (2004). [PubMed: 15556029]
3. Huang M, Hull CM, Sporulation: how to survive on planet Earth (and beyond). Curr. Genet. 63, 831–838 (2017). [PubMed: 28421279]

4. Pandey R, Ter Beek A, Vischer NOE, Smelt JPPM, Brul S, Manders EMM, Live Cell Imaging of Germination and Outgrowth of Individual Bacillus subtilis Spores; the Effect of Heat Stress Quantitatively Analyzed with SporeTracker. PLoS ONE. 8, e58972 (2013). [PubMed: 23536843]
5. Wang S, Setlow P, Li Y, Slow Leakage of Ca-Dipicolinic Acid from Individual Bacillus Spores during Initiation of Spore Germination. J. Bacteriol. 197, 1095–1103 (2015). [PubMed: 25583976]
6. Setlow P, Christie G, Bacterial Spore mRNA – What's Up With That? Front. Microbiol. 11 (2020), doi:10.3389/fmicb.2020.596092.
7. Ghosh S, Korza G, Maciejewski M, Setlow P, Analysis of Metabolism in Dormant Spores of Bacillus Species by 31P Nuclear Magnetic Resonance Analysis of Low-Molecular-Weight Compounds. J. Bacteriol. 197, 992–1001 (2015). [PubMed: 25548246]
8. Wang S, Faeder JR, Setlow P, Li Y, Memory of germinant stimuli in bacterial spores. mBio. 6, e01859–15 (2015). [PubMed: 26604257]
9. Zhang P, Liang J, Yi X, Setlow P, q. Li Y, Monitoring of Commitment, Blocking, and Continuation of Nutrient Germination of Individual Bacillus subtilis Spores. J. Bacteriol. 196, 2443–2454 (2014). [PubMed: 24769693]
10. Pedrero-López LV, Pérez-García B, Mehltreter K, Sánchez-Coronado ME, Orozco-Segovia A, Can fern spores develop hydration memory in response to priming? J. Plant Physiol. 232, 284–290 (2019). [PubMed: 30544053]
11. Brunel N, van Rossum MCW, Lapicque's 1907 paper: from frogs to integrate-and-fire. Biol. Cybern. 97, 337–339 (2007). [PubMed: 17968583]
12. Tuckwell HC, Introduction to theoretical neurobiology (1988), doi:10.1017/cbo9780511623202.
13. Burkitt AN, A Review of the Integrate-and-fire Neuron Model: I. Homogeneous Synaptic Input. Biol. Cybern. 95, 1–19 (2006). [PubMed: 16622699]
14. Setlow P, Germination of Spores of Bacillus Species: What We Know and Do Not Know. J. Bacteriol. 196, 1297–1305 (2014). [PubMed: 24488313]
15. Moir A, Cooper G, Spore Germination. Microbiol. Spectr. 3 (2015), doi:10.1128/microbiolspec.TBS-0014-2012.
16. Prindle A, Liu J, Asally M, Ly S, Garcia-Ojalvo J, Suel GM, Süel GM, Ion channels enable electrical communication in bacterial communities. Nature. 527 (2015), doi:10.1038/nature15709.
17. Larkin JW, Zhai X, Kikuchi K, Redford SE, Prindle A, Liu J, Greenfield S, Walczak AM, Garcia-Ojalvo J, Mugler A, Süel GM, Signal Percolation within a Bacterial Community. Cell Syst. 7, 137–145.e3 (2018). [PubMed: 30056004]
18. Yang C-Y, Bialecka-Fornal M, Weatherwax C, Larkin JW, Prindle A, Liu J, Garcia-Ojalvo J, Süel GM, Encoding Membrane-Potential-Based Memory within a Microbial Community. Cell Syst. 10, 417–423.e3 (2020). [PubMed: 32343961]
19. Humphries J, Xiong L, Liu J, Prindle A, Yuan F, Arjes HA, Tsimring L, Süel GM, Species-independent attraction to biofilms through electrical signaling. Cell. 168, 200–209.e12 (2017). [PubMed: 28086091]
20. Sirec T, Benarroch JM, Buffard P, Garcia-Ojalvo J, Asally M, Electrical polarization enables integrative quality control during bacterial differentiation into spores. iScience. 16, 378–389 (2019). [PubMed: 31226599]
21. Hodgkin AL, Huxley AF, A quantitative description of membrane current and its application to conduction and excitation in nerve. J. Physiol. 117, 500–544 (1952). [PubMed: 12991237]
22. Eisenstadt E, Potassium Content During Growth and Sporulation in Bacillus subtilis. J. Bacteriol. 112, 264–267 (1972). [PubMed: 4627924]
23. Whatmore AM, Chudek JA, R. H. Y. 1990 Reed, The effects of osmotic upshock on the intracellular solute pools of Bacillus subtilis. Microbiology. 136, 2527–2535.
24. Zheng L, Abhyankar W, Ouwerling N, Dekker HL, van Veen H, van der Wel NN, Roseboom W, de Koning LJ, Brul S, de Koster CG, Bacillus subtilis Spore Inner Membrane Proteome. J. Proteome Res. 15, 585–594 (2016). [PubMed: 26731423]
25. Holtmann G, Bakker EP, Uozumi N, Bremer E, KtrAB and KtrCD: Two K+ Uptake Systems in Bacillus subtilis and Their Role in Adaptation to Hypertonicity. J BACTERIOL. 185, 10 (2003).

26. Stautz J, Hellmich Y, Fuss MF, Silberberg JM, Devlin JR, Stockbridge RB, Hänelt I, Molecular Mechanisms for Bacterial Potassium Homeostasis. J. Mol. Biol., 166968 (2021). [PubMed: 33798529]
27. Lundberg ME, Becker EC, Choe S, MstX and a Putative Potassium Channel Facilitate Biofilm Formation in Bacillus subtilis. PLoS ONE. 8, e60993 (2013). [PubMed: 23737939]
28. Barfield JP, Yeung CH, Cooper TG, Characterization of potassium channels involved in volume regulation of human spermatozoa. Mol. Hum. Reprod. 11, 891–897 (2005). [PubMed: 16421215]
29. Cortezzo DE, Setlow B, Setlow P, Analysis of the action of compounds that inhibit the germination of spores of Bacillus species. J. Appl. Microbiol, 17 (2004).
30. Mancilla E, Rojas E, Quinine blocks the high conductance, calcium-activated potassium channel in rat pancreatic β-cells. FEBS Lett. 260, 105–108 (1990). [PubMed: 2404792]
31. Mitchell C, Skomurski JF, Vary JC, Effect of ion channel blockers on germination of Bacillus megaterium spores. FEMS Microbiol. Lett. 34, 211–214 (1986).
32. Lee DD, Galera-Laporta L, Bialecka-Fornal M, Moon E, Shen Z, Briggs SP, Garcia-Ojalvo J, Süel GM, Magnesium flux modulates ribosomes to increase bacterial survival. Cell (2019), doi:10.1016/j.cell.2019.01.042.
33. Cowan AE, Olivastro EM, Koppel DE, Loshon CA, Setlow B, Setlow P, Lipids in the inner membrane of dormant spores of Bacillus species are largely immobile. Proc. Natl. Acad. Sci. 101, 7733–7738 (2004). [PubMed: 15126669]
34. Moir A, Smith DA, The genetics of bacterial spore germination. Annu. Rev. Microbiol. 44, 531–553 (1990). [PubMed: 2252393]
35. Leonard AP, Cameron RB, Speiser JL, Wolf BJ, Peterson YK, Schnellmann RG, Beeson CC, Rohrer B, Quantitative analysis of mitochondrial morphology and membrane potential in living cells using high-content imaging, machine learning, and morphological binning. Biochim. Biophys. Acta BBA - Mol. Cell Res. 1853, 348–360 (2015).
36. Perez-Valdespino A, Li Y, Setlow B, Ghosh S, Pan D, Korza G, Feeherry FE, Doona CJ, Li Y-Q, Hao B, Setlow P, Function of the SpoVAEa and SpoVAF Proteins of Bacillus subtilis Spores. J. Bacteriol. 196, 2077–2088 (2014). [PubMed: 24682327]
37. Kikuchi K, Galera-Laporta L, Weatherwax C, Lam JY, Moon E, Theodorakis EA, Garcia-Ojalvo J, Suel GM, Electrochemical potential enables dormant spores to integrate environmental signals. Version 1, Zenodo (2022); 10.5281/zenodo.6967596
38. Irnov I, Winkler WC, A regulatory RNA required for antitermination of biofilm and capsular polysaccharide operons in Bacillales: Antitermination of exopolysaccharide genes. Mol. Microbiol. 76, 559–575 (2010). [PubMed: 20374491]
39. Jarmer H, Berka R, Knudsen S, Saxild HH, Transcriptome analysis documents induced competence of *Bacillus subtilis* during nitrogen limiting conditions. FEMS Microbiol. Lett. 206, 197–200 (2002). [PubMed: 11814663]
40. Sterlini JM, Mandelstam J, Commitment to sporulation in Bacillus subtilis and its relationship to development of actinomycin resistance. Biochem. J. 113, 29–37 (1969). [PubMed: 4185146]
41. Atluri S, Ragkousi K, Cortezzo DE, Setlow P, Cooperativity Between Different Nutrient Receptors in Germination of Spores of Bacillus subtilis and Reduction of This Cooperativity by Alterations in the GerB Receptor. J. Bacteriol. 188, 28–36 (2006). [PubMed: 16352818]
42. Sinai L, Rosenberg A, Smith Y, Segev E, Ben-Yehuda S, The Molecular Timeline of a Reviving Bacterial Spore. Mol. Cell. 57, 695–707 (2015). [PubMed: 25661487]
43. Rana PS, Gibbons BA, Vereninov AA, Yurinskaya VE, Clements RJ, Model TA, Model MA, Calibration and characterization of intracellular Asante Potassium Green probes, APG-2 and APG-4. Anal. Biochem. 567, 8–13 (2019). [PubMed: 30503709]
44. Garmaise DL, Paris GY, Komlossy J, Chambers CH, McCrae RC, Anthelmintic quaternary salts. III. Benzothiazolium salts. J. Med. Chem. 12, 30–36 (1969). [PubMed: 5763036]
45. Dey A, Hajra A, Metal-Free Synthesis of 2-Arylbenzothiazoles from Aldehydes, Amines, and Thiocyanate. Org. Lett. 21, 1686–1689 (2019). [PubMed: 30811211]
46. Ra CS, Jung BY, Park G, The fungicidal benzothiazole methoxyacrylates: Synthesis, conformational analysis and fungicidal activity. Heterocycles. 62, 793–802 (2004).

47. Seelam M, Shaikh BV, Tamminana R, Kammela PR, An efficient methodology for the synthesis of thioureas from amine mediated by a cobalt source. Tetrahedron Lett. 57, 5297–5300 (2016).

48. Inoue H, Konda M, Hashiyama T, Otsuka H, Watanabe A, Gaino M, Takahashi K, Date T, Okamura K, Takeda M, Narita H, Murata S, Odawara A, Sasaki H, Nagao T, Synthesis and biological evaluation of alkyl, alkoxy, alkylthio, or amino-substituted 2,3-dihydro-1,5-benzothiazepin-4(5H)-ones. Chem. Pharm. Bull. (Tokyo). 45, 1008–1026 (1997). [PubMed: 9214707]

49. Tzanopoulou S, Sagnou M, Paravatou-Petsotas M, Gourni E, Loudos G, Xanthopoulos S, Lafkas D, Kiaris H, Varvarigou A, Pirmettis IC, Papadopoulos M, Pelecanou M, Evaluation of Re and 99m Tc Complexes of 2-(4′-Aminophenyl)benzothiazole as Potential Breast Cancer Radiopharmaceuticals. J. Med. Chem. 53, 4633–4641 (2010). [PubMed: 20518489]

50. Chhabra M, Sinha S, Banerjee S, Paira P, An efficient green synthesis of 2-arylbenzothiazole analogues as potent antibacterial and anticancer agents. Bioorg. Med. Chem. Lett. 26, 213–217 (2016). [PubMed: 26590102]

Box 1.

Mathematical model of dormant spore electrophysiology

According to the processes depicted in Fig. 1F, we assume that the changes in concentrations of extracellular and intracellular potassium, K_e and K_i respectively, are governed by the flow of potassium ions through the spore membrane:

$$\frac{dK_e}{dt} = Fg_K n^4(V - V_K) + Fg_n n^4(V - V_n) - \gamma_e(K_e - K_m)$$

$$\frac{dK_i}{dt} = -Fg_K n^4(V - V_K) - Fg_n n^4(V - V_n)$$

The model includes ion flow through both specific and non-specific channels, with conductances g_K and g_n respectively. Additionally, extracellular potassium is subject to a relaxational term (third term in the right-hand side of the K_e equation) that pulls it to the concentration of potassium in the medium, K_m. Ion flow through the channels depends on the electrochemical state of the spore, given by its membrane potential V, and reversal potentials V_K and V_n corresponding to specific and non-specific ions, respectively. Crucially, the reversal potential of potassium depends on the potassium concentrations through the Nernst equation:

$$V_K = V_{K0}\ln(K_e/K_i)$$

As mentioned in the main text, the channels are assumed to open in the presence of germinant, which produces an outward flux of potassium and consequently a sudden increase in membrane potential. The dynamics of the membrane potential V and gating variable n are described in the Supplementary Text, together with the rest of the parameters and all parameter values.

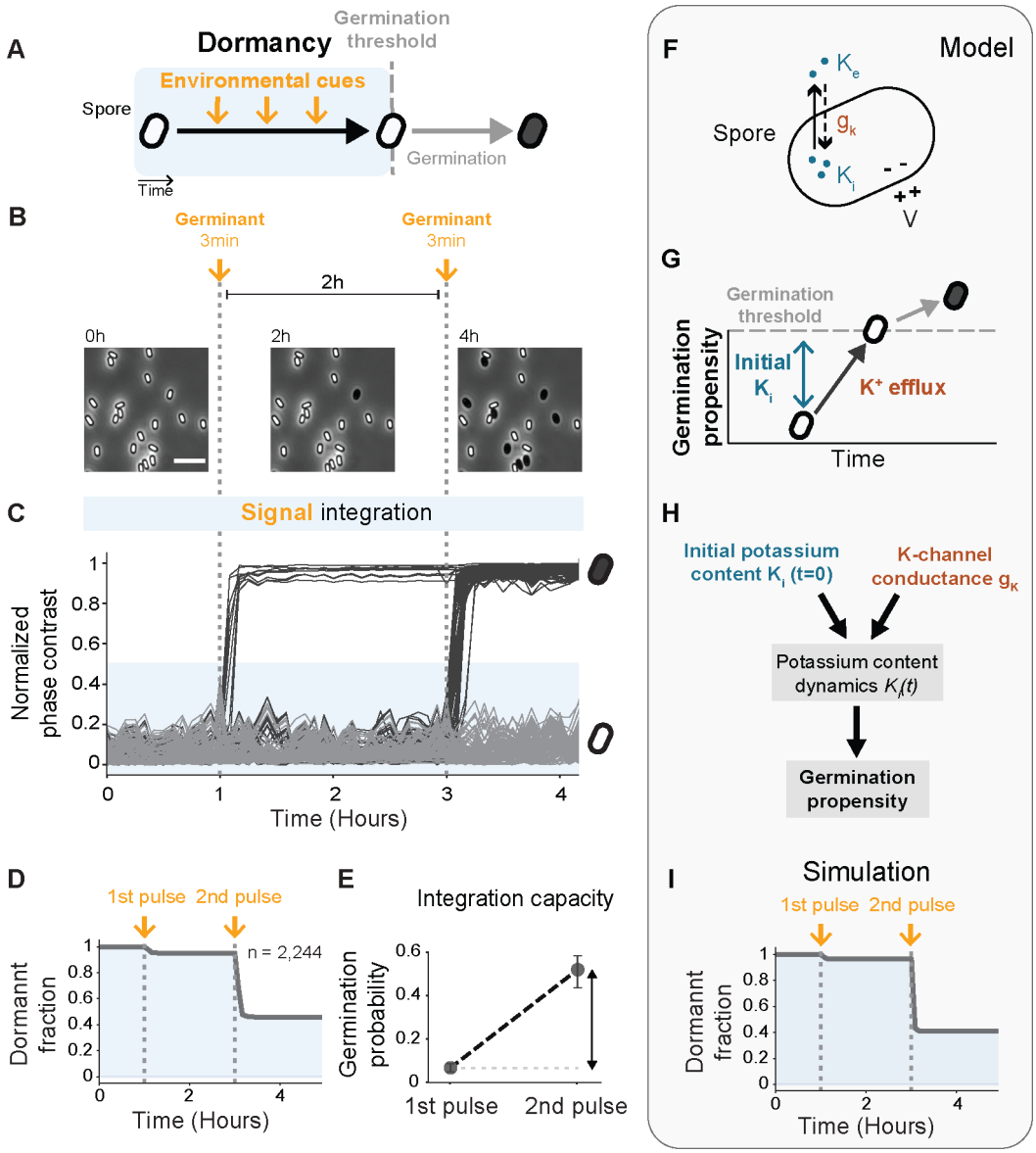

Fig. 1: *Bacillus subtilis* spores integrate over two consecutive germinant pulses.

(A) Bacterial spores can remain in dormancy (shaded area in blue) for years seemingly without any biological activity. It is thus unclear how spores sense environmental cues while dormant, and before triggering germination.

(B) Filmstrip from phase-contrast microscopy showing the fractional germination response to the pulses. Spores contained in a microfluidic chip were subjected to 3 min germinant pulses (10 mM L-alanine, dotted vertical lines) separated by 2-hour intervals. These pulses triggered germination of a subset of spores, detected by phase-contrast imaging: white dormant spores become phase dark when germinating as they rehydrate. Spores that maintain dormancy, despite exposure to germinant pulses, provoke the question of whether they can sense and process such environmental information. Scale bar indicates 5 μm.

(C) Single-cell time traces showing the change in the normalized phase-contrast intensity during spore germination (n = 200, subset of data from Fig. 1D). We note that collective fluctuations in the image intensity are due to subtle changes in camera focus.
(D) Fraction of dormant spores after each germinant pulse (n = 2,244). The abrupt decrease in the dormant fraction after the second germinant pulse indicates the ability of spores to integrate signals over consecutive pulses.
(E) The germination probability in each pulse is calculated based on the remaining dormant spores before each germinant pulse. The difference in the germination probability between the two pulses (vertical arrow) provides a metric to quantify the information integration by spores.
(F) Cartoon showing the main components of our mathematical model. The flux of potassium in a spore is assumed to depend partially on the difference between its internal (K_i) and external (K_e) concentrations, the K-channel conductance (g_k), and the membrane potential (V) of the spore. **(G)** The spore's approach to the germination threshold is dictated by initial potassium content (K_i) and potassium efflux.
(H) In the mathematical model, the initial potassium content (K_i, t = 0) and the K-channel conductance (g_k) determine the potassium dynamics in spores ($K_i(t)$). These dynamics determine the spore's propensity to germinate (See Box 1 and Supplementary Text).
(I) Simulated fraction of dormant spores after each germinant pulse.

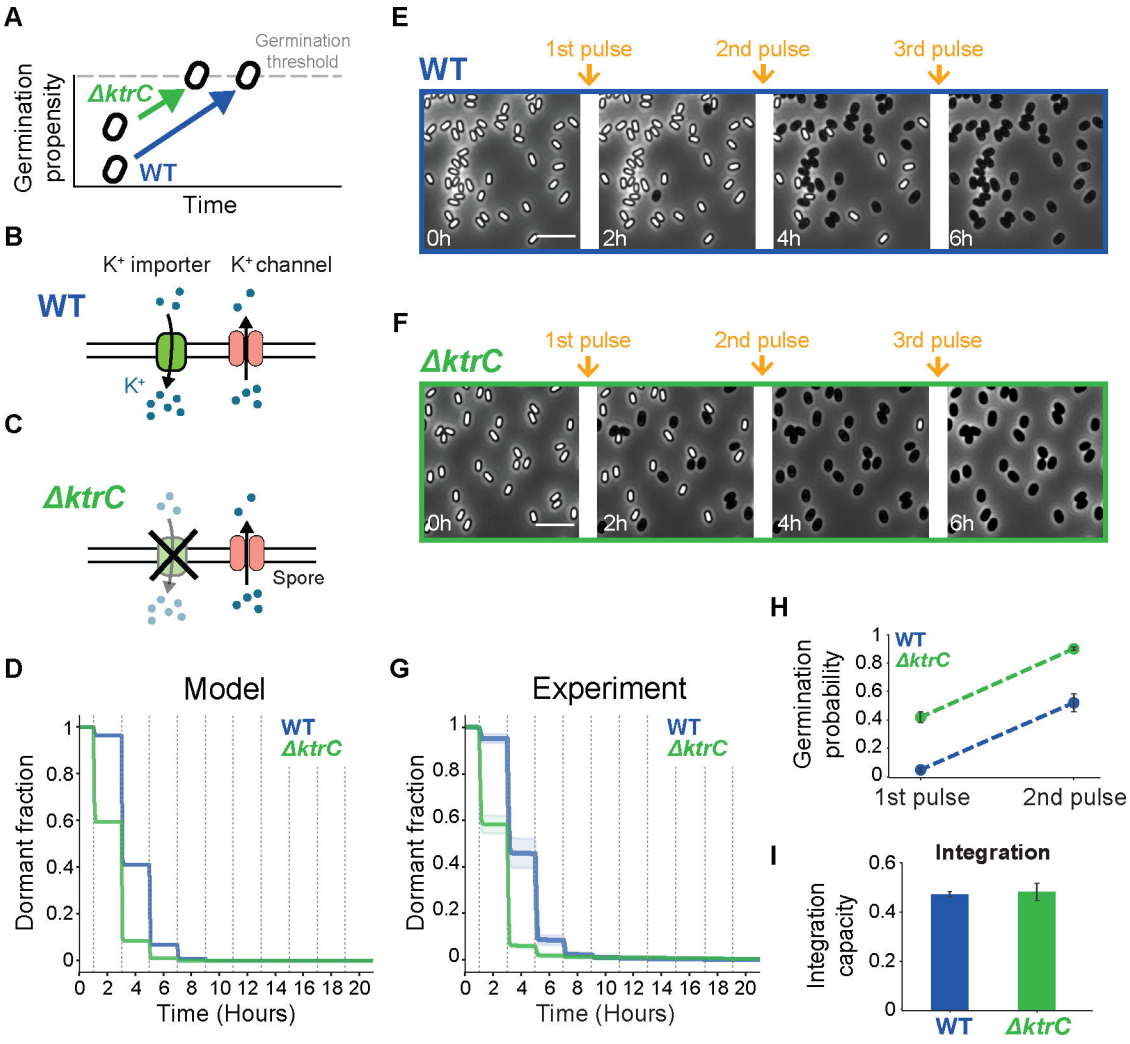

Fig. 2: Role of potassium in the germination threshold.

(A) The model predicts that the deletion of the KtrC importer reduces the distance of spores to their germination threshold. This in turn will increase the germination propensity of *ΔktrC* spores, compared to wild-type (WT) spores.

(B) Wild-type cells contain both potassium importers and ion channels.

(C) The *ktrC* mutant spores (*ΔktrC*) lack the gene for the potassium importer KtrC.

(D) Model-generated dormant fraction of the WT (blue), and the *ΔktrC* (green) strains. Dotted vertical lines indicate germinant pulses.

(E&F) Phase-contrast microscopy filmstrips for representative WT (E) and *ΔktrC* spores (F), respectively. Snapshots show spores before and after the indicated germinant pulses. Scale bars indicate 5 μm.

(G) Dormant fraction from single-cell experimental results for WT (blue, mean ± SD, n = 2,244, data from Fig. 1D), and *ΔktrC* (green, mean ± SD, n = 2,154). Dotted vertical lines indicate germinant pulses.

(H) Germination probabilities of the WT and the *ΔktrC* spores increase with consecutive pulses. Both strains reach 50% germination out of all initial spores (half-maximum germination) after two consecutive pulses. Error bars represent standard deviation.

(I) Bar plot showing the integration capacity of the WT and the *ΔktrC* strains (0.47 ± 0.01 and 0.48 ± 0.03, respectively) calculated from the differences in germination probabilities shown in panel (H). Error bars represent standard deviation.

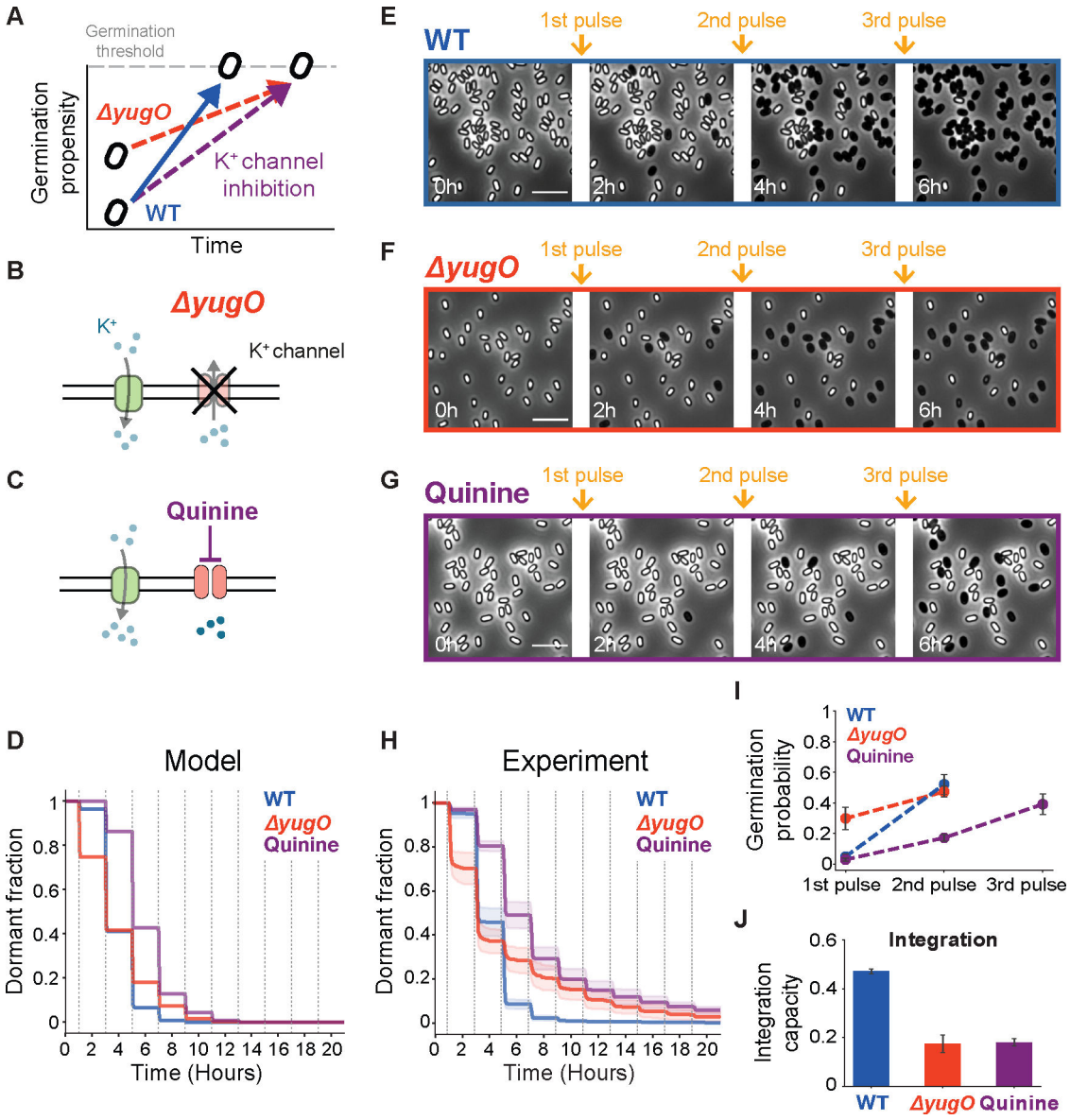

Fig. 3: Potassium ion flux underlies integration capacity of dormant spores.

(A) The *ΔyugO* mutant spores are expected to have be initially closer to the germination threshold but have slower potassium efflux, impacting their approach to the threshold. The inhibition of potassium channels in WT spores is similarly expected to impact their approach to the germination threshold.

(B) The *ΔyugO* mutant spores lack the gene for the YugO channel, which is the only known potassium-specific channel in *B. subtilis* spores.

(C) The drug quinine targets potassium channels, blocking ion efflux.

(D) Model-generated dormant fraction of WT (blue), *ΔyugO* (red), and quinine addition to WT spores (purple).

(E-G) Filmstrips for representative WT (E) and *ΔyugO* (F) spores, and WT spores in the presence of 1 mM quinine (G), respectively. Snapshots show spores before and after the indicated germinant pulses. Scale bars indicate 5 μm.

(H) The dormant fraction from single-cell measurements of WT (mean ± SD; blue, n = 2,244, data from Fig. 1D), *ΔyugO* (mean ± SD; red, n = 1,058), and 1 mM quinine addition to WT spores (mean ± SD, purple, n = 4,491).
(I) The germination probability until half-maximum germination for WT (data from Fig. 2H), *ΔyugO*, and quinine addition. The inhibition of potassium efflux reduces the germination probability, requiring three pulses to reach the half-maximum germination. Error bars represent standard deviation.
(J) The genetic and chemical inhibition of potassium efflux (*ΔyugO* and quinine addition, respectively) reduces the integration capacity of spores (WT 0.47 ± 0.01, data from Fig. 2I, *ΔyugO* 0.17 ± 0.04, and quinine 0.18 ± 0.01; mean ± SD).

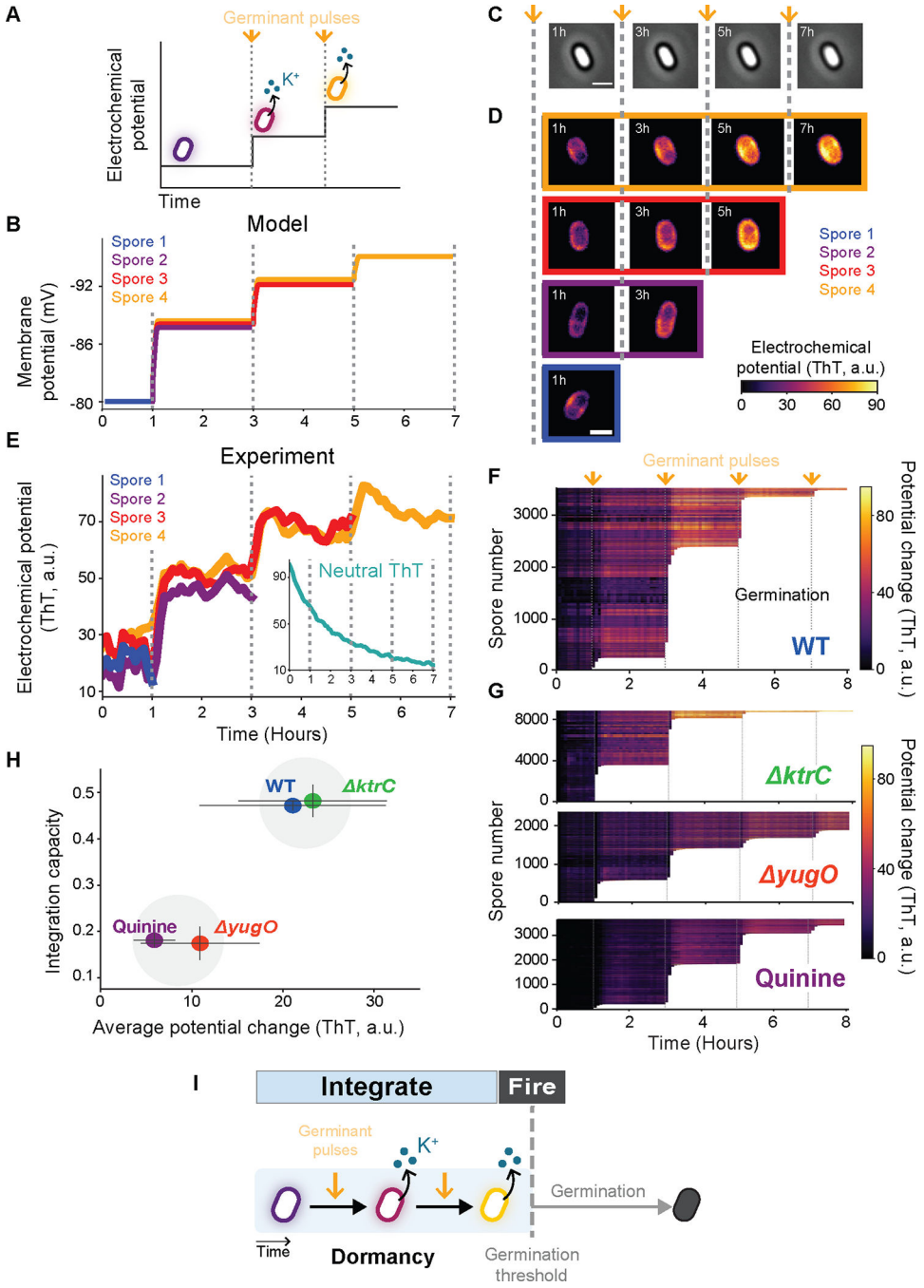

Fig. 4: Dormant spores exhibit sudden changes in their electrochemical potential, visualizing integration over germinant pulses.

(A) Cartoon illustrating the hypothesis that spores release potassium after each germinant pulse, generating a change in their electrochemical potential.

(B) Mathematically predicted stepwise membrane potential (mV) jumps when spores are exposed to germinant pulses (dotted vertical lines). Depicted are representative time traces for individual spores that germinate in response to different germinant pulse numbers. The termination of the time trace indicates germination.

(C) Phase-contrast images of a spore that remains dormant (phase bright) despite exposure to three consecutive germinant pulses. Dotted vertical lines indicate germinant pulse exposure. Scale bar indicates 1 μm.

(D) Top fluorescence filmstrip shows the color-coded electrochemical potential amplitude (ThT, a.u.) of the spore depicted in panel (C). The other three filmstrips below show individual spores, each of which germinate in response to different germinant pulses.

(E) Single-cell time traces of the electrochemical potential signal (ThT, a.u.) for the corresponding spores in Fig. 3D (see Fig. S7A for corresponding phase-contrast traces). The termination of the time traces indicates germination. The inset shows the time trace of a single spore stained with the charge-neutral ThT fluorescent dye (see Fig. S8D for data from multiple spores).

(F) Measurement of 3,484 individual WT spores showing amplitude color-coded time traces that show the changes in electrochemical potential signal (ThT, a.u.) triggered by germinant pulses (dotted vertical lines). The termination of the time trace (white region) indicates germination.

(G) Single-cell time traces of the potential change (ThT, a.u) for *ΔktrC* (n = 8,790), *ΔyugO* (n = 2,380), and WT with 1 mM quinine (n = 3,653), respectively. Each line represents a single-spore time trace until germination (white region). Germinant pulses are indicated with arrows and dotted vertical lines.

(H) Scatter plot of the integration capacity as a function of the average potential change (ThT, a.u) of all strains and conditions tested in this study: WT, *ΔktrC*, *ΔyugO*, and WT with quinine.

(I) Conceptual summary of the proposed integrate-and-fire mechanism. Spores integrate germinant exposure information over time through efflux of potassium ions. The resulting change in electrochemical potential drives them towards a germination threshold. Spores that reach the threshold “fire” the germination program which is marked by the abrupt change in phase-contrast refractility.